



A System Dynamics Approach to Model Photosynthesis at Leaf Level Under Fluctuating Light

Nicole Salvatori^{1,2*}†, Fabrizio Carteni^{3†}, Francesco Giannino³, Giorgio Alberti^{1,4}, Stefano Mazzoleni^{3,5} and Alessandro Peressotti¹

¹ D14A, Department of Agri-Food, Environmental and Animal Sciences, University of Udine, Udine, Italy, ² Department of Life Sciences, University of Trieste, Trieste, Italy, ³ Department of Agricultural Sciences, University of Naples Federico II, Portici, Italy, ⁴ Faculty of Science and Technology, Free University of Bolzano, Bolzano, Italy, ⁵ Task Force on Microbiome Studies, University of Naples Federico II, Naples, Italy

OPEN ACCESS

Edited by:

Zhong-Hua Chen,
Western Sydney University, Australia

Reviewed by:

Alfred Holzwarth,
Max Planck Institute for Chemical
Energy Conversion, Germany
Alessandro Alboresi,
University of Padua, Italy

*Correspondence:

Nicole Salvatori
nicole.salvatori@phd.units.it

† These authors have contributed
equally to this work

Specialty section:

This article was submitted to
Plant Biophysics and Modeling,
a section of the journal
Frontiers in Plant Science

Received: 01 October 2021

Accepted: 24 December 2021

Published: 28 January 2022

Citation:

Salvatori N, Carteni F, Giannino F,
Alberti G, Mazzoleni S and
Peressotti A (2022) A System
Dynamics Approach to Model
Photosynthesis at Leaf Level Under
Fluctuating Light.
Front. Plant Sci. 12:787877.
doi: 10.3389/fpls.2021.787877

Photosynthesis has been mainly studied under steady-state conditions even though this assumption results inadequate for assessing the biochemical responses to rapid variations occurring in natural environments. The combination of mathematical models with available data may enhance the understanding of the dynamic responses of plants to fluctuating environments and can be used to make predictions on how photosynthesis would respond to non-steady-state conditions. In this study, we present a leaf level System Dynamics photosynthesis model based and validated on an experiment performed on two soybean varieties, namely, the wild type Eiko and the chlorophyll-deficient mutant MinnGold, grown in constant and fluctuating light conditions. This mutant is known to have similar steady-state photosynthesis compared to the green wild type, but it is found to have less biomass at harvest. It has been hypothesized that this might be due to an unoptimized response to non-steady-state conditions; therefore, this mutant seems appropriate to investigate dynamic photosynthesis. The model explained well the photosynthetic responses of these two varieties to fluctuating and constant light conditions and allowed to make relevant conclusions on the different dynamic responses of the two varieties. Deviations between data and model simulations are mostly evident in the non-photochemical quenching (NPQ) dynamics due to the oversimplified combination of PsbS- and zeaxanthin-dependent kinetics, failing in finely capturing the NPQ responses at different timescales. Nevertheless, due to its simplicity, the model can provide the basis of an upscaled dynamic model at a plant level.

Keywords: modeling, photosynthesis, Chl-deficient, soybean, system dynamics

INTRODUCTION

The continuous rise in population requires an increase in agricultural production of at least 60% (Alexandratos and Bruinsma, 2012). By being the source of food and responsible for the survival of the majority of life on Earth (Stirbet et al., 2020), photosynthesis has recently become a target to improve global food production, since the increase in genetic yield potential seems to be

hindered (Foyer et al., 2017; Taylor and Long, 2017). Photosynthesis has been intensively studied in laboratories, but, due to its complex nature, it still provides some challenges (Flexas et al., 2012). Mathematical models can provide a different tool to better understand the dynamics of this process and can be used to make predictions on how photosynthesis would respond to limiting situations (Stirbet et al., 2020).

Several modeling efforts have been done in order to describe photosynthesis as a whole. The models can be differentiated by considering the processes at steady-state (Farquhar et al., 1980; Buckley et al., 2003; Ye et al., 2013) or non-steady-state (Kirschbaum et al., 1997; Morales et al., 2018; Bellasio, 2019; Nedbal and Lazàr, 2021); for their spatial scale, i.e., leaf scale (Farquhar et al., 1980; Zhu et al., 2013; Viallet-Chabrand et al., 2017a) or canopy scale (Song and Zhu, 2012); and for the different modeling approaches, i.e., empirical models (Viallet-Chabrand et al., 2017a), system biology models (Pettersson and Ryde-Pettersson, 1988; Zhu et al., 2013; Kannan et al., 2019), and process-based models (Kirschbaum et al., 1997; Morales et al., 2018; Bellasio, 2019).

The processes of photosynthesis have been initially tackled simulating steady-state conditions (Farquhar et al., 1980; Von Caemmerer, 2013). These models are fundamental in understanding the physiological characteristics and answering very specific questions, but usually overestimate total photosynthesis in fluctuating environmental conditions (Timm et al., 2004). In fact, external conditions are rarely stable in natural environments, so plants need to continuously adjust to optimize the carbon uptake in these dynamic conditions (Kaiser et al., 2018). Different adjustments can be operated by plants depending on the time scale considered (Kono and Terashima, 2014): in the fast temporal scale, plants respond by regulating the mechanisms involved in photochemical (Kono and Terashima, 2014; Kaiser et al., 2018) and non-photochemical processes (Acebron et al., 2021), activating the Calvin Cycle enzymes (Porcar-Castell et al., 2006) and moving their chloroplasts within the leaves (Kaiser et al., 2015); slower adjustments can then be due to the regulation of the stomata (Buckley, 2017; Viallet-Chabrand et al., 2017b; Matthews et al., 2018), the movements of the leaves within the canopy (as photonastic movements or due to the wind), and the adaptative adjustments in nitrogen and chlorophyll content (Posada et al., 2009; Zhang et al., 2016).

Among the main variable conditions, the most relevant is light. Light intensity is continuously changing due to the movements of the clouds and to the wind moving the leaves (Percy, 1990; Retkute et al., 2015). Plants need to adapt to these changes in light conditions, and some species may be more efficient than others in doing it (Kromdijk et al., 2016; Urban et al., 2017; Matsubara, 2018). One rising question is if a reduction in chlorophyll content might be detrimental or beneficial when dealing with fluctuating light conditions. At a canopy level, the role of chlorophyll content has been investigated (Ort et al., 2015; Slattery et al., 2016; Gu et al., 2017; Walker et al., 2018), and it has been proposed that a reduced chlorophyll content would entail a better distribution of the light in the lower layers of the canopy, therefore increasing the overall photosynthesis.

Nevertheless, few studies have analyzed the effect of chlorophyll reduction in fluctuating environments (Ferroni et al., 2020).

In this study, we focused on the effect of fluctuating light on two soybean varieties, namely, the green wild type soybean (Eiko) and a chlorophyll-deficient mutant (MinnGold), which has been first described by Campbell et al. (2015). It has been shown that MinnGold has comparable light curves and A/Ci curves (steady-state measurements) at leaf level compared with Eiko, but lower biomass was found at harvest (Sakowska et al., 2018). It was hypothesized that a slower adjustment to fluctuating light might cause a lower carbon accumulation at a canopy level and that steady-state measurements at leaf level would not be able to capture this difference (Genesio et al., 2020).

Therefore, in this study, we reported the investigation of the role of the chlorophyll content in adjusting to light fluctuations, combining experimental observations with a modeling framework. To begin with, we implemented a model at leaf level to be a basis in understanding the response of these two varieties to highly fluctuating light environments. We decided to use a process-based approach, based on the principles of System Dynamics, according to which a complex system can be represented by flows, compartments (stocks), and feedback loops (Forrester, 1971).

MATERIALS AND METHODS

Two soybean varieties have been used in this study with different chlorophyll contents, namely, Eiko, the green cultivar used as the wild type and MinnGold, the chlorophyll-deficient mutant (Campbell et al., 2015; Sakowska et al., 2018). The plants were sown in 3 L pots and grown inside a controlled growth chamber system (Salvatori et al., 2021) for 5 weeks with either non-fluctuating light or fluctuating light conditions. The light was turned on from 5:00 to 19:00 h, and the intensity was set to simulate the daily profile of the sun, reaching a maximum of $650 \mu\text{mol m}^{-2} \text{s}^{-1}$ for the non-fluctuating light protocol or fluctuating every minute (1 min high-light and 1 min low-light) with an amplitude of $\pm 20\%$ around the non-fluctuating light intensity value (**Supplementary Figure 1**). By doing this, all plants received the same amount of light throughout the day. In each chamber, we placed a ceptometer at the level of the pots to continuously measure the transmitted light (tPPFD); we also measured the albedo every 2–3 days. Therefore, by knowing the incident light (PPFD), we estimated the absorbed light (aPPFD) by the canopy as $\text{aPPFD} = \text{PPFD} - \text{rPPFD} - \text{tPPFD}$, where $\text{rPPFD} = \text{PPFD} \cdot \text{albedo}$. Therefore, the absorption coefficients ($\alpha = \text{aPPFD}/\text{PPFD}$) were estimated as 0.78 and 0.54 for Eiko and MinnGold, respectively.

Next, three plants from each variety and each light protocol were randomly chosen as replicates, from which we selected a young and fully expanded leaf to perform fluorescence analysis combined with gas exchange using the LI-6800 (Licor Biosciences, Nebraska, United States) equipped with infrared gas analyzers (IRGA) coupled with pulse-amplitude modulation (PAM) fluorometer. In particular, we were interested in recording the carbon assimilation (A), the electron transport rate (ETR), and the non-photochemical quenching (NPQ).

We used the following protocol: all plants were dark-adapted overnight, then the light was turned on following either a constant light protocol for 60 min at $650 \mu\text{mol m}^{-2} \text{s}^{-1}$ or a fluctuating light protocol with light intensity changing from 780 to $520 \mu\text{mol m}^{-2} \text{s}^{-1}$ every minute by simulating the growth conditions. These levels of light intensity were chosen to avoid saturating photosynthetic photon flux (Sakowska et al., 2018) in order to prevent photoinhibition. The CO_2 levels were maintained at 400 ppm, vapor pressure deficit (VPD) was kept at 1.8 kPa, and leaf temperature was kept at 25°C .

The carbon assimilation rate (A in $\mu\text{mol CO}_2 \text{ m}^{-2} \text{ s}^{-1}$) was calculated as follows:

$$A = \frac{\mu_0 \left[c_0 - c_a \left(\frac{1-w_0}{1-w_a} \right) \right]}{s}$$

where μ_0 is the flow rate ($\mu\text{mol air s}^{-1}$) entering the leaf chamber, s is the leaf area (m^2), c_0 and w_0 are the CO_2 and H_2O concentrations (in $\mu\text{mol CO}_2$ and $\text{mmol H}_2\text{O}$, respectively) entering the leaf chamber, and c_a and w_a are the CO_2 and H_2O concentrations exiting the chamber.

Throughout the protocol, a saturating light pulse of $> 5,000 \mu\text{mol m}^{-2} \text{s}^{-1}$ was given to the leaf sample for 800 ms every 30 s, to quantify maximal fluorescence in the light (F'_m) and dark (F_m). Each of these flashes lasts 0.8 s and added 20% to the total flux seen by the plants, arriving at an actual average illumination of approximately $800 \mu\text{mol m}^{-2} \text{s}^{-1}$. The operating efficiency of the PSII (Φ_{PSII}) was calculated as follows (Genty et al., 1989):

$$\Phi_{PSII} = \frac{(F'_m - F_s)}{F'_m}$$

where F_s is the steady-state fluorescence.

NPQ was calculated using the equation from Bilger and Björkman (1990) based on the Stern-Volmer method, as follows:

$$NPQ = \frac{(F_m - F'_m)}{F'_m}$$

Finally, the ETR was calculated based on Krall and Edwards (1992), as follows:

$$ETR = I \cdot \alpha \cdot fraction_{PSII} \cdot \Phi_{PSII}$$

where I is the incident light, $fraction_{PSII}$ is the fraction of absorbed light that is received by the PSII and is normally set to 0.5 (Baker, 2008), α is the absorbance coefficient which was set to 0.55 for MinnGold and 0.78 for Eiko as previously shown.

Model Description

In this study, we presented a model of the main processes involved in the regulation of the photosynthesis of leaves of C3 plants exposed to fast changes of light intensity. **Figure 1** shows a schematic diagram of the model structure with a simplified representation of the implemented processes, within the complex phenomena occurring in photosynthesis.

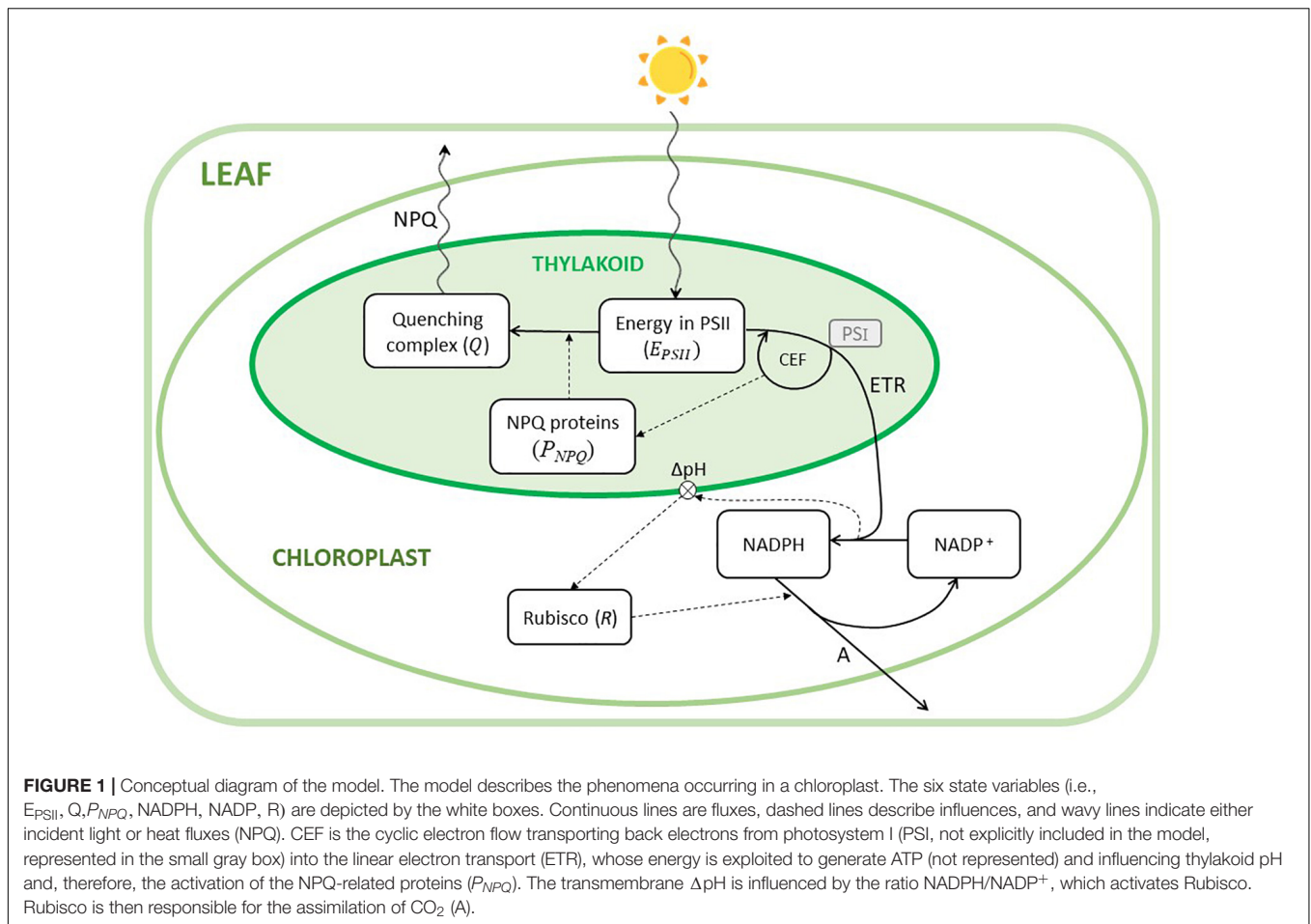
For the sake of simplicity, the model essentially considers the main dynamics of a single chloroplast as representative of a whole leaf, in a sort of “big chloroplast” approach. We did

not explicitly model the limitations due to stomatal conductance. This assumption is reasonable since the modeled leaf is exposed to optimal conditions of CO_2 and average light intensity. Even if this dynamic becomes relevant during the induction phase (dark-light transition), it is known that, in soybean, this limitation can be mainly attributed to Rubisco activation (Soleh et al., 2016, 2017; Taylor and Long, 2017). Furthermore, the two varieties did not show any statistical differences in the dynamic of the stomatal conductance (**Supplementary Figure 2**).

Here, we focused on the limitations imposed by the light reactions. In fact, rapid light fluctuations would not have a direct drastic effect on the Calvin-Benson cycle, because the activation/deactivation of the enzymes under fluctuations of light takes several minutes (Yamori, 2016) and, therefore, the activation level would depend on the average intensity, independently from fluctuations shorter than a few minutes. Furthermore, in low light, photosynthesis is restricted by the light absorption of the light harvesting systems (Long and Bernacchi, 2003; Li et al., 2021). When light excites the photosystem 2 (PSII), many pigments (chlorophyll *a* and *b* antenna proteins) collect this energy and transfer it to the reaction center. This number of pigments can be variable from plant to plant and determine the ability of the photosystem to transfer this energy. PSII oxidizes water to O_2 releasing protons into the lumen. The electrons are then passed on to the Cytochrome b6f (Cyt b6f) which delivers them to photosystem 1 (PSI) transporting additional protons into the lumen. This proton pumping from the stroma into the lumen creates a pH gradient (ΔpH) (Flexas et al., 2012). For simplicity, these last processes involving Cyt b6f and PSI are not included in the model (even if their role at steady-state has been established; Johnson and Berry, 2021) and, therefore, not represented in **Figure 1**.

The energy transported is used to reduce the final acceptor NADP^+ to NADPH. The ΔpH generated is then used by the ATP synthase to produce ATP as protons diffuse back from the lumen to the stroma. This process is generally called linear electron flow (LEF; in **Figure 1** defined as ETR), and the chemical energy produced (ATP and NADPH) is used in the Calvin Cycle to fix CO_2 . The Calvin Cycle is regulated by the enzyme Rubisco, which is itself activated by the changing in the ΔpH generated by the electron transport. Generally, the rate of CO_2 fixation at a steady-state has been described by the model of Farquhar et al. (1980) and Farquhar and Von Caemmerer (1982) as the minimum of the rate of carboxylation under the limitation of Rubisco activity and of RuBP regeneration. In this work, the limitation by Rubisco is explicitly included, whereas the limitation of RuBP regeneration is assumed as proportional to the rate of oxidation of NADPH to NADP^+ .

When there is an excess of energy, this can be dissipated through several processes, which are called NPQ. These mechanisms involve several processes that are differentiated on the time scale of their relaxation kinetics (Müller et al., 2001): a fast phase is assigned to qE (i.e., energy-dependent quenching), which relaxes within seconds to minutes (Krause et al., 1982); two middle phases qZ (i.e., zeaxanthin-dependent component) detectable within 10–15 min



(Nilkens et al., 2010) and qT (i.e., state transition quenching) in 30 min and a slow phase qI in the time scale of an hour (Kohzuma and Hikosaka, 2018).

We only modelled the energy-dependent quenching (qE) since it is the most important component of NPQ when regarding fluctuating irradiance; in fact, by operating in the scale of minutes (Ebenhöh et al., 2014), it responds most quickly to changes in light intensities (Kaiser et al., 2015). qE is regulated by luminal pH and the xanthophyll cycle pigments. The saturation of the dark reactions causes a decrease in the luminal pH, causing the protonation of some PSII proteins (PsbS proteins) (Matuszyńska et al., 2016), the release of violaxanthin molecules and their de-epoxidation to antheraxanthin and zeaxanthin. Zeaxanthin then binds to PSII proteins (in which PsbS proteins have been protonated), forming a quenching complex favoring the dissipation of the excitation energy as heat (Porcar-Castell et al., 2006). PsbS dynamics are more relevant in the fast fluctuations of light, whereas zeaxanthin activation is related to the induction phase of photosynthesis. For the sake of simplicity, we did not distinguish between the two former processes, which have been combined. Furthermore, the generation of a ΔpH is necessary under environmental stressful conditions, when the dark reactions are saturated, allowing the production of ATP without the reduction of

NADP⁺ (Roach and Krieger-Liszkay, 2014). In such cases, the cyclic electron flow (CEF) around the PSI is activated, increasing electron transfer from PSI to the plastoquinone pool, and again to PSI via the Cyt b6/f complex (Yamori, 2016). In C3 plants, CEF is considered negligible at steady-state conditions, thus becoming relevant under specific stressful conditions such as low CO₂, high light, drought, or during the dark-to-light transitions (Rochaix, 2011). CEF then becomes a regulator of NPQ and ETR at non-steady-state conditions (Roach and Krieger-Liszkay, 2014; Yamori, 2016).

Mathematical Formulation of the Model

In the model, the described processes are represented as a set of differential equations representing the dynamics of 6 state variables: the energy in PSII (E_{PSII}), the activation level of the NPQ-related proteins (P_{NPQ}), the quenching complex of P_{NPQ} with the PSII (Q), the dynamics of NADPH and NADP⁺, and the activation level of Rubisco (R) (Figure 1).

The first variable represents the excitation energy of PSII. When the photosystem receives a light input, the excitation energy is transferred either as linear electron transport (ETR), regulated by the amount of the final acceptor NADP⁺ or as dissipation of energy, regulated by P_{NPQ} . P_{NPQ} combines the dynamics of the zeaxanthin activation and the PsbS protonation.

The following equation describes these processes:

$$\frac{dE_{PSII}}{dt} = \underbrace{\alpha \cdot c_{in} \cdot PAR \cdot \left(1 - \frac{E_{PSII}}{E_{PSII}^*}\right)}_{\text{Energy input}} - \underbrace{v_{ETR} \cdot E_{PSII} \cdot NADP^+}_{\text{ETR}} - \underbrace{v_d \cdot E_{PSII} \cdot P_{NPQ} \cdot \left(1 - \frac{Q}{Q^*}\right)}_{\text{Energy dissipation}} \quad (1)$$

The energy input is formulated as a logistic equation—since the photosystem can hold a maximum amount of energy (E_{PSII}^*) that depends on the amount of chlorophylls present—with a velocity of induction c_{in} which is linearly related to the absorption coefficient (α) and the photosynthetically active radiation (PAR) (**Table 1**). The linear electron transport is linearly related to the energy in PSII (E_{PSII}) and to the amount of $NADP^+$ in the chloroplast stroma, with a velocity of induction v_{ETR} .

Then the excess energy in PSII can be dissipated only if zeaxanthin has formed the quenching complex with the PSII protonated (Q). This complex is then able to release energy as heat (NPQ). The dynamics of the quenching complex of P_{NPQ} with PSII are described as follows:

$$\frac{dQ}{dt} = v_d \cdot E_{PSII} \cdot P_{NPQ} \cdot \left(1 - \frac{Q}{Q^*}\right) - \underbrace{v_{NPQ} \cdot Q}_{\text{NPQ}} \quad (2)$$

The energy dissipation flux has an upper limit described by the saturation term of the quenching complex ($1 - Q/Q^*$) and a velocity of induction v_d . The energy released as heat (NPQ) is then linearly related to Q with a velocity of induction v_{NPQ} .

The activation level of the P_{NPQ} is then related to the cyclic electron transport (CEF) as follows:

$$\frac{dP_{NPQ}}{dt} = \begin{cases} \underbrace{v_p \cdot (1 - P_{NPQ})}_{\text{Protein activation}} & \text{if } CEF > c_y \\ 0 & \text{if } CEF \leq c_y \end{cases} \quad (3)$$

with

$$CEF = \underbrace{\alpha \cdot c_{in} \cdot PAR \cdot \left(1 - \frac{E_{PSII}}{E_{PSII}^*}\right)}_{\text{Energy input}} - \underbrace{v_{ETR} \cdot E_{PSII} \cdot NADP^+}_{\text{ETR}}$$

The values of P_{NPQ} are assumed to range from 0 (inactive) to 1 (fully active). P_{NPQ} is modeled with a saturating curve whose formation depends on CEF . In fact, as previously described, the activation of the proteins related to NPQ is triggered by a strong change in luminal pH, which occurs when a decoupling of the light reactions with the dark reactions generates an excess in energy that is exploited by the cyclic electron transport (CEF) to produce a decrease in the luminal pH as well as a production of ATP.

Finally, the energy flowing from PSII to PSI (ETR) is used to reduce $NADP^+$ to $NADPH$ whose dynamics are described as

follows:

$$\frac{dNADPH}{dt} = \underbrace{v_{ETR} \cdot E_{PSII} \cdot NADP^+}_{\text{ETR}} \cdot \eta_{NADP^+} - \underbrace{v_C \cdot R \cdot NADPH}_{\text{A}} \cdot \eta_{NADPH} \quad (4)$$

$$\frac{dNADP^+}{dt} = - \frac{dNADPH}{dt} \quad (5)$$

The two η parameters represent the efficiencies of the linear electron transport in producing $NADPH$ (η_{NADP^+}) and consuming $NADP^+$ (η_{NADPH}). In particular, the parameter η_{NADPH} regulates the velocity of the Calvin Cycle and, therefore, can be related to the RuBP regeneration. Equation 6 describes the dynamics of $NADP^+$ just as opposed to the one of $NADPH$. Carbon assimilation (A) is, therefore, regulated by the rate of carboxylation (v_C) mediated by Rubisco (R). The dynamics of Rubisco activation is described by the following equation:

$$\frac{dR}{dt} = \underbrace{v_R \cdot (1 - R)}_{\text{Rubisco activation}} \cdot \min(d, \Delta pH) \quad (6)$$

with

$$\Delta pH = \frac{NADPH}{NADP^+}$$

R is modeled with a saturating curve whose formation depends on the change of transmembrane ΔpH , which can be accounted as the ratio between $NADPH$ and $NADP^+$ (derived by Morales et al., 2018). The parameter d represents the maximum value of ΔpH allowing for a smoother curve in the first phases of the activation of the Rubisco.

The description of the six state variables and the parameters with the relative units are found in **Table 1**. The model allows the characterization of three quantities measured in gas exchange and fluorescence analysis: ETR , A , and NPQ . These three quantities are fluxes ($\mu\text{mol m}^{-2} \text{s}^{-1}$) and can be derived from the described equations: $ETR = v_{ETR} \cdot E_{PSII} \cdot NADP^+$ from Equation 1, $NPQ = v_{NPQ} \cdot Q$ from Equation 2, and $A = v_C \cdot R \cdot NADPH$ from Equation 4.

Sensitivity Analysis

A local sensitivity analysis (Norton, 2015) was performed to analyze the model behavior under parameter perturbation. The normalized sensitivity index is calculated by changing each parameter of $\pm 5\%$ while keeping all the other constant. The equation for the sensitivity index is the following:

$$SSE_{i,\Delta} = \sqrt{\frac{1}{3 \cdot n} \sum_{j=1}^3 \sum_{i=1}^n \left(\frac{X^j(p_1, p_2, \dots, p_i + \Delta, \dots, p_k) - X^j(\mathbf{p})}{\max(X^j(\mathbf{p})) - \min(X^j(\mathbf{p}))} \right)^2} \quad (7)$$

where $SSE_{i,\Delta}$ is the standardized elementary effect of the parameter p_i with Δ ($\pm 5\%$) perturbation on model outputs and k is the number of parameters (equal to 13); $X^j(\mathbf{p})$ are the simulated values of the j -th quantity considered (i.e., NPQ , ETR ,

TABLE 1 | State variables, fixed parameters, and calibrated parameters of the model.

	Symbol	Description	Units	Value	
				Eiko	MinnGold
State variables	E_{PSII}	Energy in photosystem II ($t = 0$)	$\mu\text{mol m}^{-2}$	0	
	Q	Quenching complex ($t = 0$)	$\mu\text{mol m}^{-2}$	0	
	P_{NPQ}	Activation level of the NPQ-related proteins ($t = 0$)	–	0	
	$NADP^+$	$NADP^+$ in chloroplast stroma ($t = 0$)	–	5	
	$NADPH$	$NADPH$ in chloroplast stroma ($t = 0$)	–	5	
Fixed parameters	R	Rubisco activation level ($t = 0$)	–	0.001	
	PAR	Photosynthetically active radiation	$\mu\text{mol m}^{-2}\text{s}^{-1}$	520 or 780	
Calibrated parameters	α	Absorption coefficient	–	0.78	0.54
	C_{in}	Energy input coefficient	–	0.23	0.25
	E_{PSII}^*	PSII energy carrying capacity	$\mu\text{mol m}^{-2}$	157.56	9.98
	V_{ETR}	Velocity of ETR	s^{-1}	0.78	11.56
	V_d	Velocity of energy dissipation	s^{-1}	0.08	7.00
	Q^*	PSII-zeax complex energy carrying capacity	$\mu\text{mol m}^{-2}$	0.07	0.03
	V_{NPQ}	Velocity of NPQ	s^{-1}	70.58	53.87
	V_p	Maximum velocity of NPQ-related proteins activation	s^{-1}	0.07	0.01
	V_C	Maximum velocity of Calvin Cycle reactions	s^{-1}	11.75	13.04
	η_{NADPH}	Efficiency of $NADPH$	–	5.07	4.10
	η_{NADP^+}	Efficiency of $NADP^+$	–	0.89	0.75
	V_R	Maximum velocity of Rubisco activation	s^{-1}	$8.9 \cdot 10^{-4}$	$14 \cdot 10^{-4}$
	d	Maximum ΔpH balance value	–	8.40	3.69
	C_y	Minimum necessary cyclic electron flow	–	–4	0

and A) without any parameter perturbation (as given in **Table 1**); and n is the number of samples per observed quantity (equal for three quantities considered).

RESULTS

Experimental Data

The model has been tested on fluorescence data coupled with gas exchange data in the fluctuating light regime for the two varieties, namely, Eiko and MinnGold. As described in the “Materials and Methods” section, the leaf was kept in the dark and then illuminated with fluctuating light at 520 and 780 $\mu\text{mol m}^{-2} \text{s}^{-1}$ for 60 min. In particular, the changes in electron transport (ETR), carbon assimilation (A), and NPQ were recorded (**Figure 2**).

After illumination, ETR and A show an initial slow photosynthetic induction (slower for MinnGold) mainly caused by the activation of the enzyme Rubisco (Soleh et al., 2016; Taylor and Long, 2017) in which the fluctuations in light are not causing, initially, corresponding fluctuations in these quantities. When Rubisco is fully activated, a steady-state is reached, and the fluctuations become more evident and constant throughout the experimental period (the last 30 min). Regarding NPQ , a faster rise of this quantity is evident with an increase in the amplitude of fluctuations in time connected to the increased level of NPQ-related proteins. **Figure 2B** focuses on a smaller experimental period when a steady-state is already being reached (from 45 to 55 min). MinnGold results are more responsive to fluctuations of light, in the sense that the changing in light intensity is causing

higher amplitudes of oscillations in ETR and, to a smaller extent, to A . In NPQ , it can be observed the opposite behavior, with fluctuations of light causing smaller amplitudes of oscillations.

Model Fitting

For the wild type Eiko (**Figure 3**), the model accurately represented the measured dynamics with an R^2 of 0.98 for ETR and A of 0.94 for NPQ . In this case, the model captured both the slow induction dynamics and the fast fluctuating dynamics.

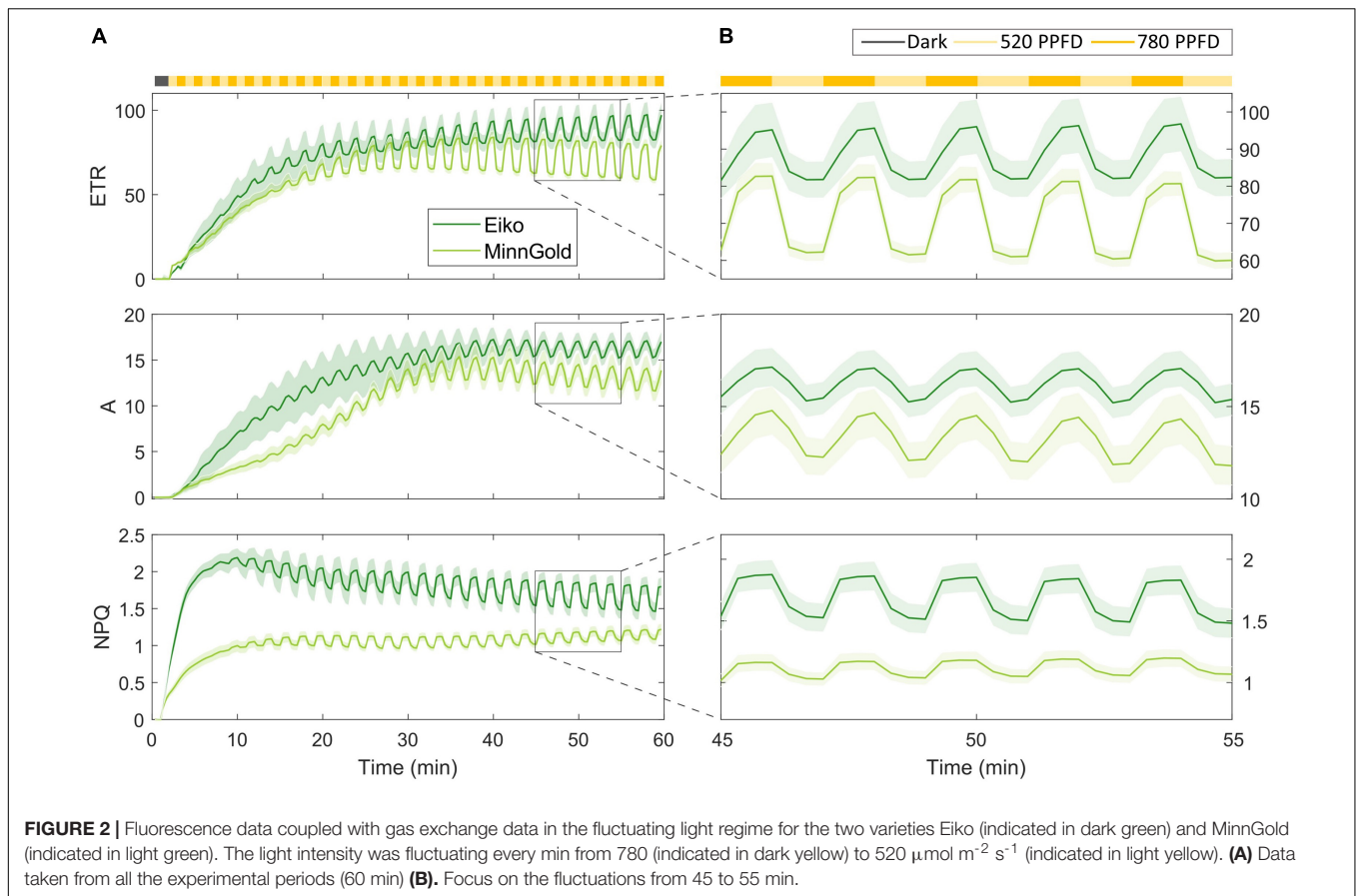
In the case of MinnGold (**Figure 4**), the model performed well for both ETR and NPQ ($R^2 = 0.93$ and 0.91 , respectively), whereas it did not capture the slow induction found in A , still having a good $R^2 = 0.84$.

Validation

The model has been then validated on gas exchange data in the constant light regime. To validate it, the model has been tested over the data using the parameters found for the fluctuating light protocol in Eiko (**Figure 5**) and MinnGold (**Figure 6** and **Table 1**). The model performed well also in these conditions, in particular for ETR ($R^2 = 0.96$ and 0.98 for Eiko and MinnGold, respectively) and A ($R^2 = 0.94$ and 0.78), with a slight underperformance for NPQ ($R^2 = 0.65$ and 0.76).

Sensitivity

The local sensitivity analysis (Equation 8) allowed identifying the parameters whose change mainly affected the three quantities considered (i.e., A , ETR , and NPQ). By changing the parameters by 5%, the outcome of the model never deviates more than 4%



from the baseline simulation (Figure 7). This means that the model is robust and not much dependent on the changes in the parameters; furthermore, no matter if the percentage change is positive or negative, the outcome is the same.

The sensitivity also showed differences in MinnGold and Eiko. In both cases, the parameter more sensible to changes is c_{in} , the parameter identifying the energy input in PSII and, therefore (with α , the absorbance coefficient), the energy entering the photosystem. Differences among MinnGold and Eiko can be found for E_{pPSII}^* , the carrying capacity of the PSII. A small difference for the two species can also be found for the parameters v_{NPQ} , E_Z^* , and v_d .

Theoretical Evaluation of the Model

The model was further validated by performing some theoretical simulations by considering Eiko parameters (Table 1). We evaluated how the three quantities (i.e., ETR , A , and NPQ) would behave when changing the period of the fluctuating light. Figure 8A shows an example of the effect of three different fluctuating periods (i.e., 30 s, 1 min, and 4 min fluctuating period with duty cycle equal to 0.5) when compared with the constant light regime. When calculating the cumulative values at steady-state (after 40 min), A and ETR resulted higher than those for constant light (fluctuating period equal to zero) when light fluctuates with a period higher than 30 s and lower than 20 min (Figure 8B).

Nevertheless, we have the opposite behavior for NPQ . We also calculated modeled cumulative steady-state values with MinnGold parameters (Supplementary Figure 3). Steady-state values of ETR and A decreased as the fluctuation period increased, except for short fluctuating periods in which they increase (of the same order as Eiko, Figure 8B). Nevertheless, in this case, we found fluctuations causing a much smaller change in NPQ steady state.

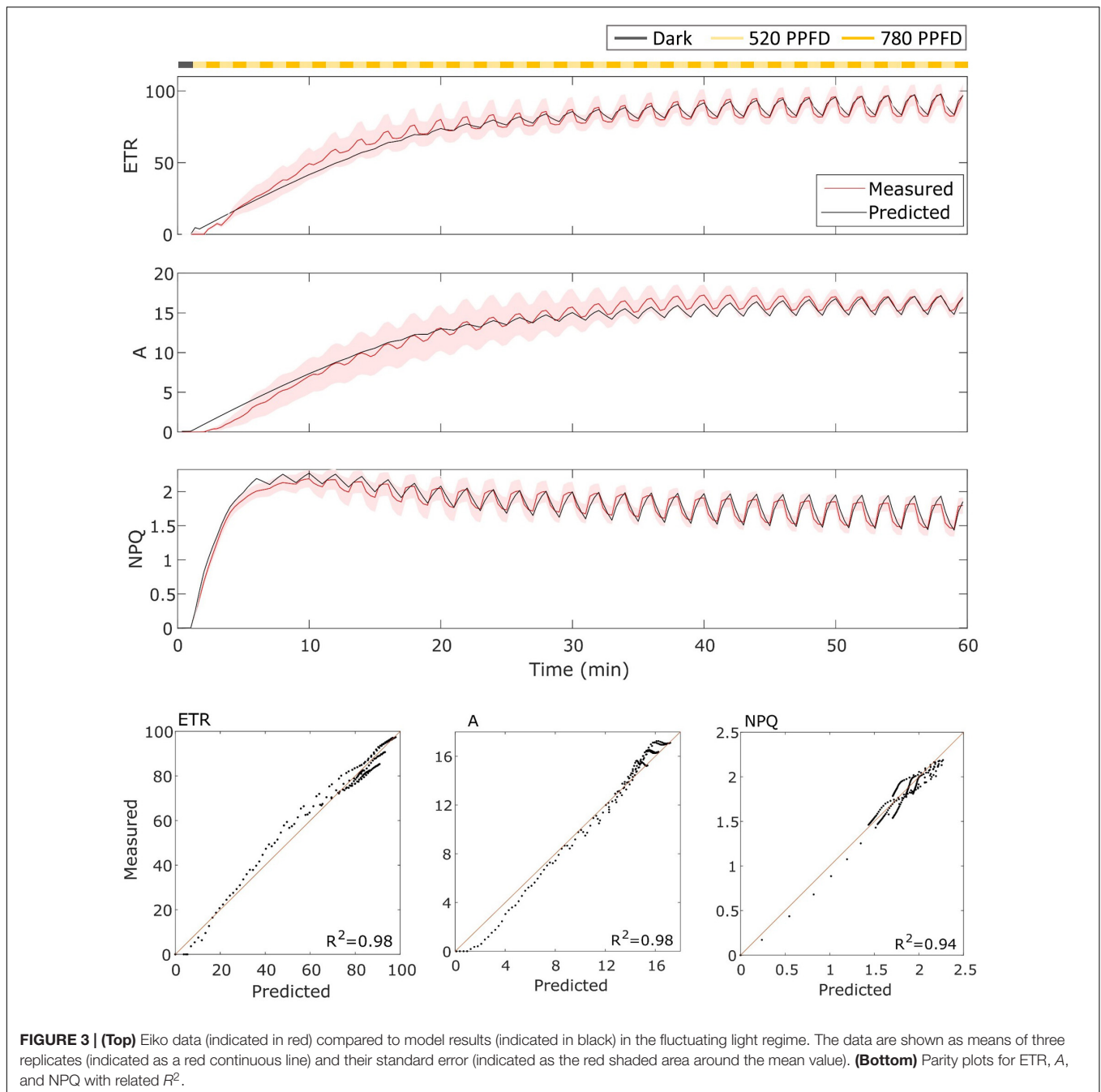
We finally performed simulations with higher fluctuations intensity, with the same fluctuating period (1-min period) (Supplementary Figure 4). In this case, the constant regime results always higher than the fluctuating regime; therefore, the higher the fluctuation amplitude, the lower would be the steady-state value.

DISCUSSION

Model Assumptions

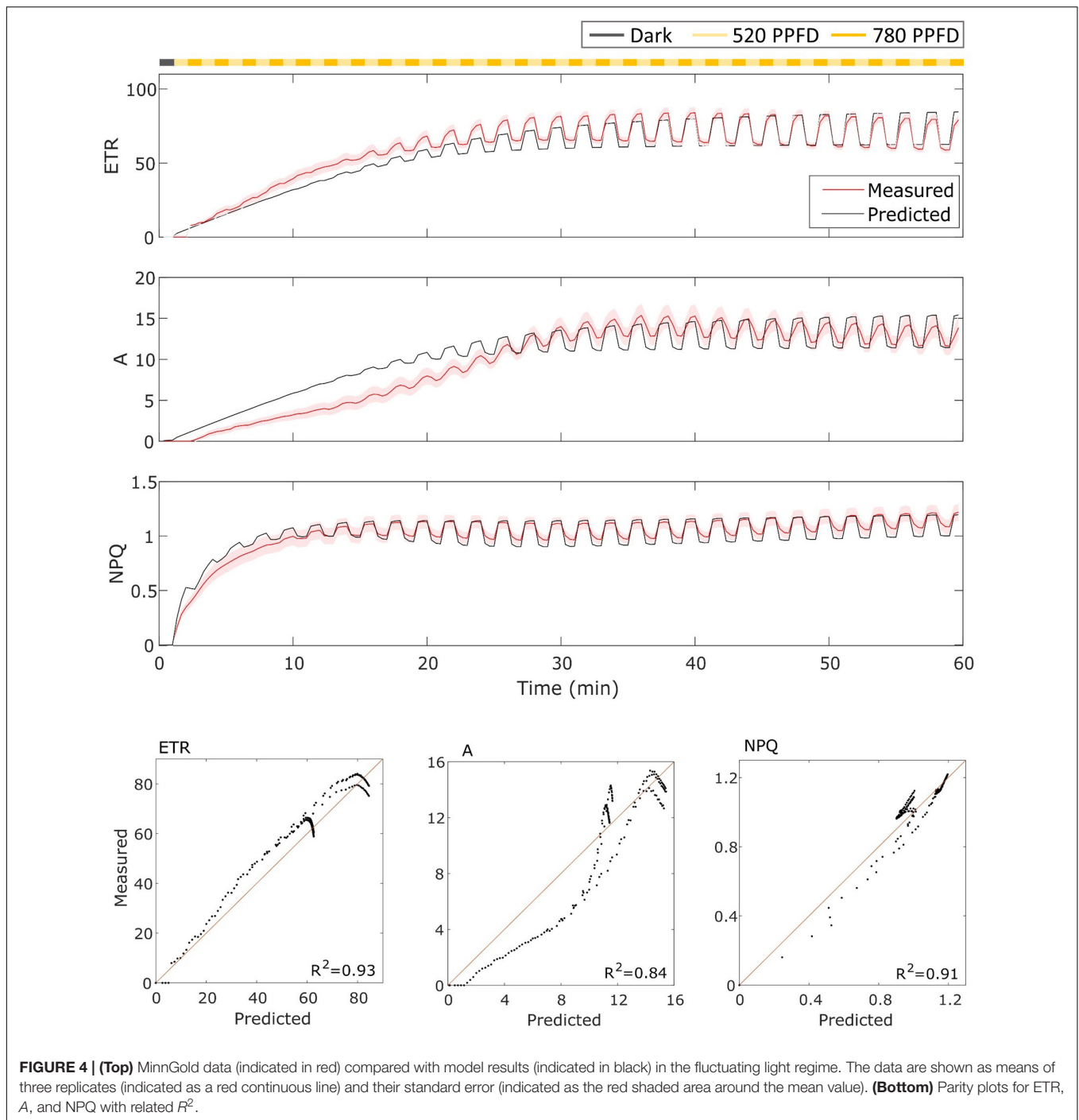
Here we presented a leaf level System Dynamics photosynthesis model based and validated on an experiment performed on two soybean varieties, namely, the wild type Eiko and the chlorophyll-deficient mutant MinnGold, grown in constant and fluctuating light conditions.

The model was developed to reflect the assumptions of the experimental conditions. Leaves were exposed to optimal CO_2



conditions and average light intensity; therefore, we assumed no limitation due to stomatal conductance. Two main conditions are investigated: (1) the photosynthetic induction during the dark-light transition and (2) the fluctuations of light maintaining the system in a continuous non-steady-state condition. One of the main results of this work is found in the modeling of the cyclic electron transport, which is thought to be fundamental in the triggering of NPQ when ETR is still limited by the downstream reactions of the Calvin Cycle (Cornic and Baker, 2012; Yamori and Shikanai, 2016). In fact, the dissipation of energy through NPQ is possible when zeaxanthin forms a quenching complex

with PSII and PsbS proteins that have been protonated. These two processes are both triggered by a change in ΔpH which, when ETR is limiting, is caused by the cyclic electron transport. The fact that NPQ activation is possible also when ETR is not fully active is evident from the data, both in the long-term and in the short-term. **Figure 2A** in fact shows that NPQ reaches a steady-state much faster than ETR and A during the dark-light transition. This is also evident in the short term: in fact, during the fluctuations of light (**Figure 2B**) at steady-state, NPQ is still found to be faster than the other quantities in reaching the steady-state associated with the specific light intensity.



We only modeled the qE component of NPQ due to the time scale of the measurements, though also qT and qI (to a lesser extent, due both to the time scale and light intensity) can act, as modeled by Ebenhöf et al. (2014). Furthermore, the generation of the energy-dependent NPQ is modeled as a single process. Though it is known that at least two different quenching sites contribute to NPQ (Nilkens et al., 2010): the PsbS-dependent located in detached antenna complexes (LHCII) and the zeaxanthin-dependent (qZ) located in smaller

antenna proteins that remain attached to the reaction center (Holzwarth and Jahns, 2014). Both processes are pH-dependent (Matuszyńska et al., 2016) and operate independently from each other. In our case, for the sake of simplicity, we have combined them in the variable named P_{NPQ} (Equation 3).

Finally, the local sensitivity analysis has demonstrated that the model is robust to changes in parameter values since a small change in the input parameters does not produce unexpected and unrealistic changes in the model outcome

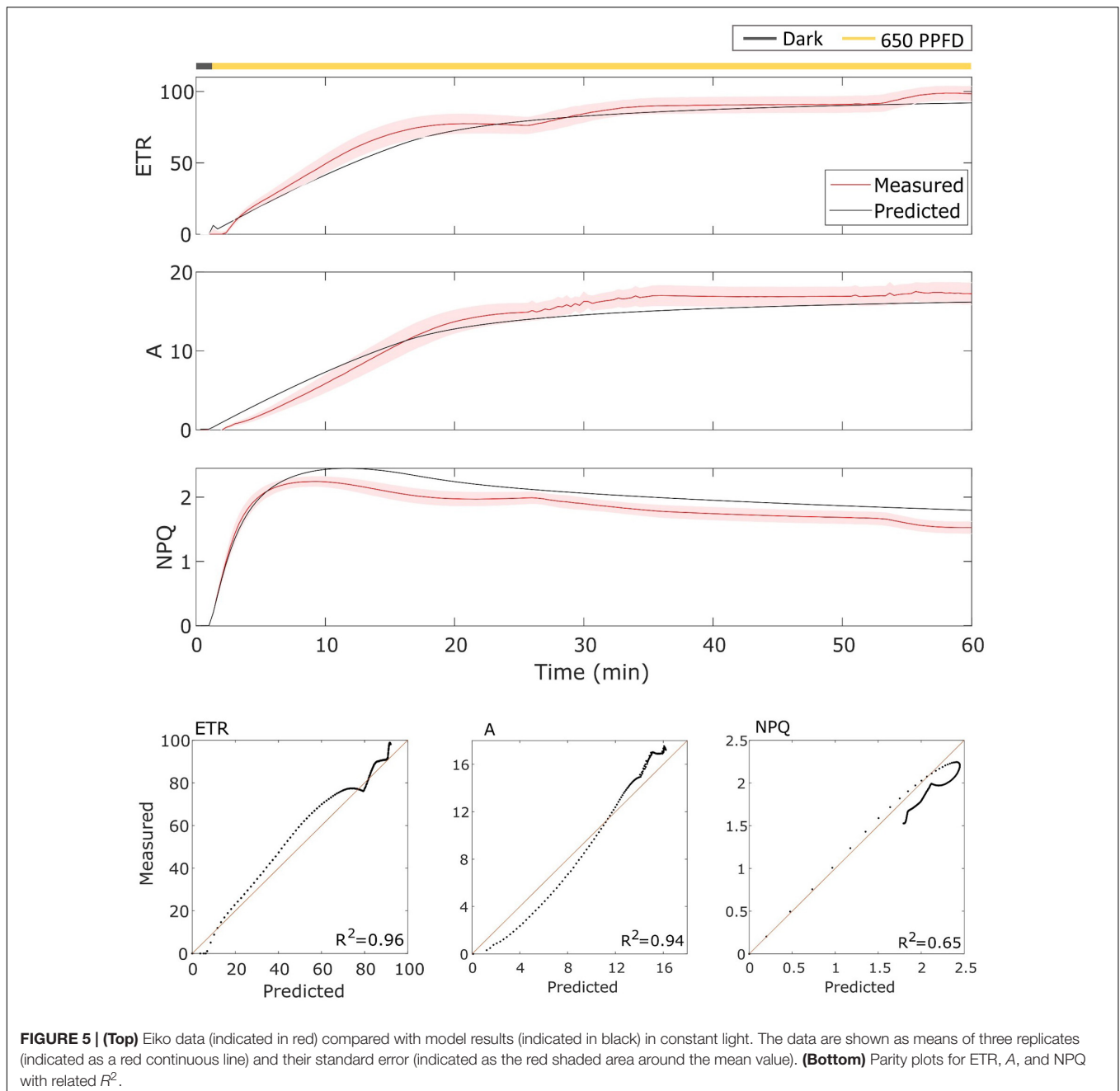


FIGURE 5 | (Top) Eiko data (indicated in red) compared with model results (indicated in black) in constant light. The data are shown as means of three replicates (indicated as a red continuous line) and their standard error (indicated as the red shaded area around the mean value). **(Bottom)** Parity plots for ETR, A, and NPQ with related R^2 .

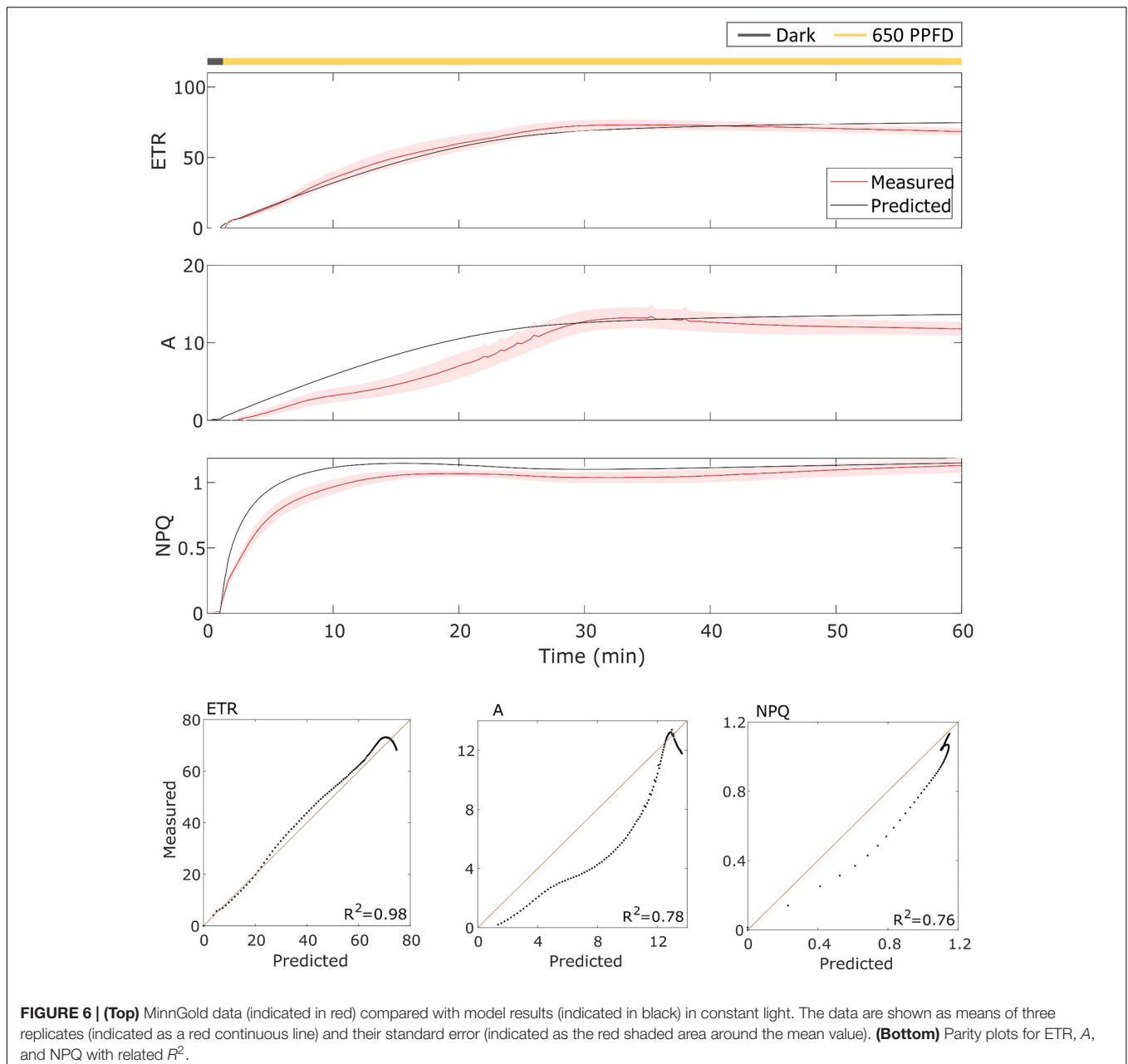
(Figure 7; Saltelli et al., 2004). Furthermore, it enables to identify the parameters which mostly influence the model outcome (in this case, c_{in} and E_{PSII}^*) and that are species-specific.

Model Performance

The model was able to simulate the experimental data reasonably well both in constant and fluctuating light conditions and in both soybean varieties with R^2 ranging from 0.65 to 0.98 (Figures 3–6). Nevertheless, two main observations were not well-fitted by the model, in addition to some finer details.

First, in MinnGold, it is found a decoupling of A and ETR in the velocity of induction in both fluctuating (Figure 4) and

constant (Figure 6) light conditions. At a steady-state, the two processes are known to be coupled, since the electron chain starts when electrons are reducing $NADP^+$, which are in turn mainly produced by the Calvin Cycle. In our model, in fact, higher ETR generates more NADPH (Equation 4), which in turn activates carbon assimilation (A). This framework, though, does not take into account photosynthetic control mechanisms *via* Cyt b6f activity (Johnson and Berry, 2021) as well as various photoprotective mechanisms to prevent photoinhibition (Yamori, 2016). Furthermore, it is known that electrons can also be transferred to other enzymes involved in the regulation of carbon metabolism as well as in nitrogen and sulfur metabolism

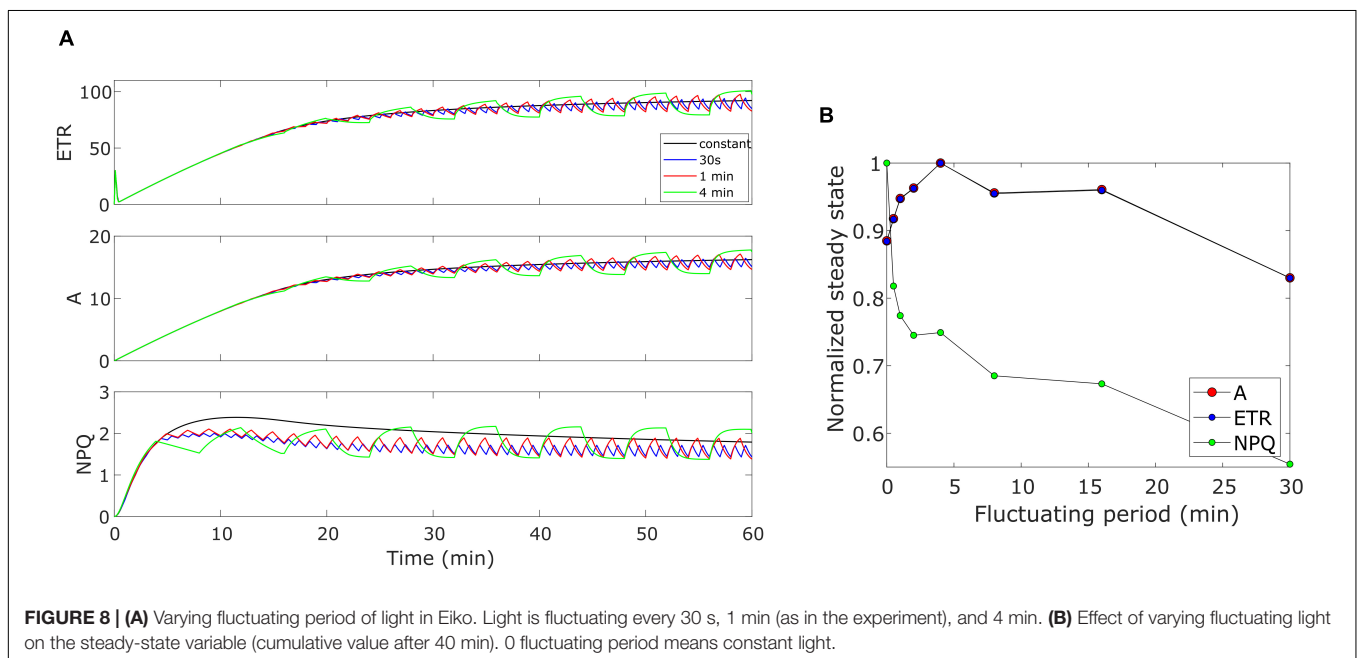
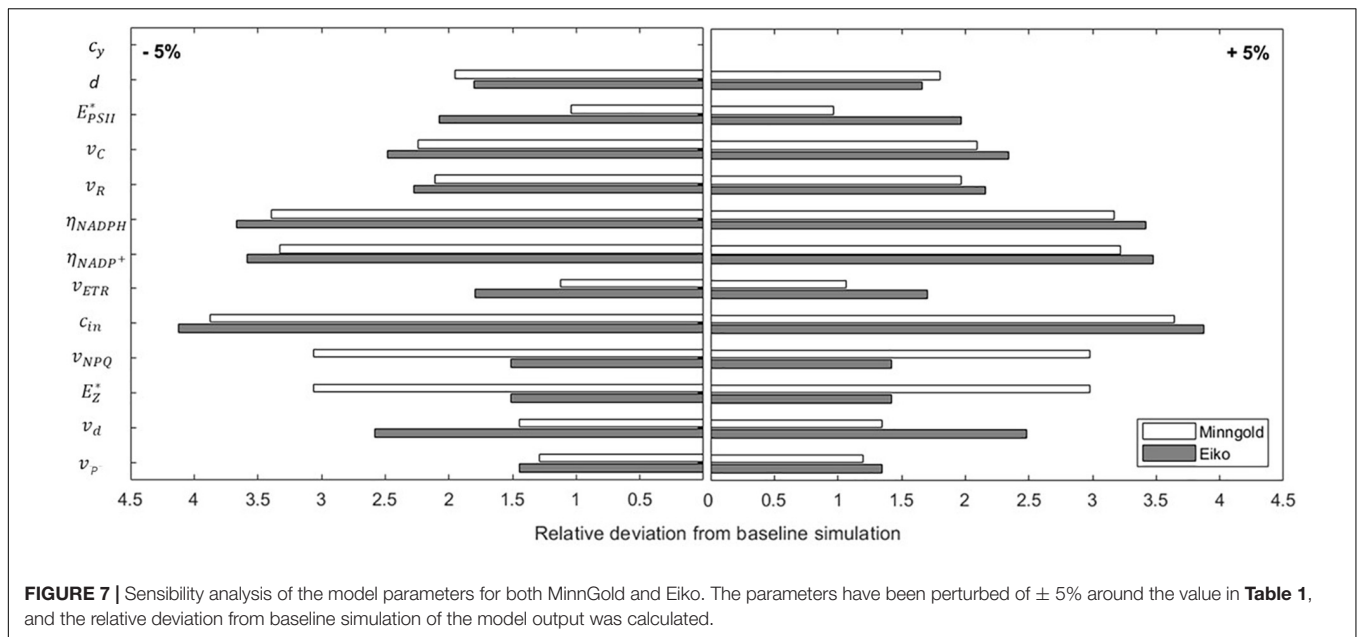


(Cornic and Baker, 2012). Nevertheless, we think that this decoupling is due to the fundamental assumptions for calculating *ETR* based on fluorescence. In fact, it is assumed that the fraction of absorbed light that is directed to PSII and the leaf absorbance are constant in the *ETR* (Baker, 2008), whereas this might not be generally true during the induction dynamics and for Chl-deficient varieties. Since this would need a further discussion and a focus on the nature of this result, we did not aim to capture this dynamic.

The second observation differing from the model is found in *NPQ* steady-state when calculated in constant light. The model in fact overestimated the steady-state values in both Eiko and MinnGold (Figures 5, 6). This might be an adaptation strategy.

Since the constant regime is less stressful for the plants, it might be that less energy needs to be dissipated as heat. Since the model was calibrated to the fluctuating light data, a stressful condition, it might be that the parameters regulating *NPQ* are set higher than necessary for the constant regime. To capture this difference, it would be probably necessary to introduce a framework regarding the adaptation of the plants based on their growing conditions.

Then, concerning only the fluctuating light part, the model simulated signal changes slower than those measured for Eiko (Figure 3) and faster for MinnGold (Figure 4) for all the three considered quantities. Regarding *NPQ*, the observed deviations can be attributed to the simplified modeled mechanisms of



generation of NPQ, which in turn regulates ETR. Indeed, two different processes have been identified to contribute to NPQ induction and relaxation dynamics: a fast one that requires the generation of a proton gradient sensed by PsbS and a slow one that is activated by low luminal pH that triggers de-epoxidation of violaxanthin to zeaxanthin (Matuszyńska et al., 2016). These two different quenching sites (PsbS-dependent, Q1; and zeaxanthin-dependent, Q2) determine four different NPQ states of PSII, which can be distinguished upon illumination of dark-adapted leaves (the so-called 4-state 2-site model of NPQ; Holzwarth and Jahns, 2014). These four states are characterized by the different velocities of activation/deactivation of the two quenching sites.

In these experiments, we expected the following: dark-adapted leaves are in the state I in which Q1 and Q2 sites are inactive; as soon as the light is turned on, the Q1 site is activated by the ΔpH (state II); after 10–20 min upon illumination, Q2 is activated by the low pH (state III); once established, Q2 remains active for a longer time; therefore, high-frequency transitions from high to low light would relax only Q1. In fact, relaxation dynamics of Q1 occur in the order of 1–2 min, that is, the same as the frequency range used in the fluctuations of light in the experiment.

The oversimplified model combines the two kinetics occurring during photosynthetic induction and light fluctuations, causing

the observed deviations between experimental data and model simulations (Figures 3–6). As it has been modelled, NPQ responses during the first induction phase and at steady state with light fluctuations are always slower in Eiko (Figure 3) and faster in MinnGold (Figure 4) compared to experimental data. Therefore, it would be necessary to explicitly include a second variable to represent both PsbS- and zeaxanthin-related processes in further developments of the model in order to describe all the different NPQ states and to capture more finely these described dynamics. Finally, the theoretical analysis of the model allowed making some relevant conclusions. When calculating the cumulative values at steady-state using Eiko's parameters in respect to different fluctuating light periods (Figure 8B), we found A and ETR steady-state values increased by reaching a maximum at 5 min fluctuating period and then to decrease for fluctuating periods longer than 20 min. Therefore, it seems that a certain range of fluctuations of light is favorable for the cumulative steady-state carbon assimilation, coherent with the observations of Graham et al. (2017). This behavior is confirmed with MinnGold parameters (Supplementary Figure 3), but in this case, we found much smaller changes in NPQ steady-state, meaning probably that NPQ relaxation dynamics in MinnGold are faster than those in Eiko, this being opposed to what proposed by Sakowska et al. (2018). More in general, the understanding of the NPQ influence in regulating dynamic photosynthesis is still controversial. Two recent articles have in fact found an opposite trend in biomass accumulation when accelerating NPQ relaxation time (Kromdijk et al., 2016; Garcia-Molina and Leister, 2020).

By being a theoretical mathematical model, when referring to the values of the parameters, it is relevant to look at the relative differences among the varieties, whereas the absolute values might not be always coherent with the biology. This is though due to the calibration procedure in finding local minima; therefore, other combinations of parameters are possible. Nevertheless, when looking at Table 1, almost all parameters are found to be comparable among the two varieties, confirming the robustness of the model. Only three parameters, namely, E_{PSII}^* , v_{ETR} , and v_d , differ. E_{PSII}^* identifies how much energy can be held by the PSII and it represents the number of chlorophyll molecules in the chloroplast, which is known to be different for Eiko and MinnGold (Slattery et al., 2017; Sakowska et al., 2018). This parameter value, therefore, is reasonably much higher in Eiko than in MinnGold. Nevertheless, v_{ETR} and v_d are the velocities of activation of ETR and NPQ, respectively, and are higher in MinnGold. This can be explained by the fact that even if MinnGold has a much lower number of chlorophyll molecules, this number is sufficient to have a responsive ETR and NPQ, which can sustain comparable carbon assimilation. In particular, both the model and the experimental data show MinnGold to be even more responsive to fluctuations of light; in fact, the fluctuating light causes higher oscillations in ETR and A (Figure 2).

Comparison With Other Models

The model presented focuses on the limitations imposed by light reactions, due to the nature of the experiment

conducted; therefore, the downstream regulation is much simplified. The model, therefore, is neither as comprehensive as preceding models (Morales et al., 2018; Bellasio, 2019) nor as detailed as other molecular models (Zhu et al., 2013; Nedbal and Lazár, 2021), but, even with its limitations, it demonstrated that a macro representation of the processes is still able to capture well the dynamics found in photosynthesis and helps in unraveling gas exchange and fluorescence data. Furthermore, the model focuses on low-intensity fluctuations of light in order to avoid photoinhibition and to stress photosynthesis due to fluctuations of light only. Nevertheless, the photoinhibitory component of NPQ (qI) or ROS production could be added in the further development of this model to deal with higher light intensities.

The main drawbacks of the model are due to the combination of the two NPQ kinetics (PsbS- and zeaxanthin-dependent), causing the presence of deviations between experimental data and model outcomes during the induction phase and the fast fluctuations of light at steady-state. The representation of both kinetics by two separate variables would allow a more appropriate description of the two existing dynamics operating at different time scales, with expected higher accordance of the model simulations with data.

Nevertheless, since the limited number of equations and related parameters, this model could become one of the building blocks of a photosynthesis model at higher scales, both leaf and canopy. Since there are already other system dynamics models, following the same procedure, focused on the dark reactions (Kirschbaum et al., 1997) and on stomatal conductance (Violet-Chabrand et al., 2016), it would be interesting to combine the presented model with these existing ones to simulate the most dynamic environmental conditions and allowing for an upscaling. In fact, even if relevant canopy level photosynthesis models exist (van der Tol et al., 2009; Song and Zhu, 2012), none, to our knowledge, aims to capture the responses of photosynthesis to dynamic environmental conditions, since it would be too complicated with the available tools. In fact, by focusing on non-steady-state conditions, we think that it is necessary to provide a more simplified representation of the system: we aim not to explain the measurements but to create a tool able to reproduce the observed dynamics, and due to its simple formulation, to apply the model to bigger scales.

CONCLUSION

In this study, we presented and validated a new system dynamic model based on the light reactions of photosynthesis. Since plants are normally dealing with dynamic environmental conditions, it should be considered to introduce into models such processes in photosynthesis that are usually discarded in steady-state models, such as the cyclic electron transport (that we represented in this model), and many other processes, such as the water-water cycle, the malate shuttle, and the other components of NPQ

(Yamori, 2016), which become limiting when conditions are unsteady.

To further address finer details of the observed dynamics, it would be necessary to introduce further experimental analysis to unravel the dynamics of LHCII, the PsbS protein, and thylakoid lipids (Nilkens et al., 2010; Jahns and Holzwarth, 2012; Ruban and Wilson, 2021) and to distinguish between various components of excess energy dissipation (Holzwarth and Jahns, 2014; Chukhutsina et al., 2019). In the case of MinnGold, a quantitative characterization of photosynthetic pigment analyses is necessary since only qualitative data are now available. These data would allow further refinement of the model. Furthermore, a more detailed description of the different NPQ dynamics will allow a better performance of the model.

Finally, even if the proposed model is at the leaf level, due to its simplicity, it could easily be one of the building blocks of a more comprehensive photosynthetic model at a plant or even canopy scale. Upscaling both the models and the experiments is fundamental since translating these short-term leaf scale results into the field is not straightforward (Kaiser et al., 2018; Matsubara, 2018). In particular, in this case, we found fluctuations of light to not interfere in the performance of MinnGold in such a short-term analysis even if it is hypothesized that they might have an effect in the long-term. Therefore, canopy level data and models become fundamental in unraveling dynamic photosynthetic processes.

REFERENCES

- Acebron, K., Matsubara, S., Jedmowski, C., Emin, D., Muller, O., and Rascher, U. (2021). Diurnal dynamics of nonphotochemical quenching in *Arabidopsis* npq mutants assessed by solar-induced fluorescence and reflectance measurements in the field. *New Phytol.* 229, 2104–2119. doi: 10.1111/nph.16984
- Alexandratos, N., and Bruinsma, J. (2012). *World Agriculture Towards 2030/2050: The 2012 Revision*. Rome: FAO.
- Baker, N. R. (2008). Chlorophyll fluorescence: a probe of photosynthesis in vivo. *Annu. Rev. Plant Biol.* 59, 89–113. doi: 10.1146/annurev.arplant.59.032607.092759
- Bellasio, C. (2019). A generalised dynamic model of leaf-level c3 photosynthesis combining light and dark reactions with stomatal behaviour. *Photosynth. Res.* 141, 99–118. doi: 10.1007/s11120-018-0601-1
- Bilger, W., and Björkman, O. (1990). Role of the xanthophyll cycle in photoprotection elucidated by measurements of light-induced absorbance changes, fluorescence and photosynthesis in leaves of *Hedera canariensis*. *Photosynth. Res.* 25, 173–185. doi: 10.1007/BF00033159
- Buckley, T. N. (2017). Modeling stomatal conductance. *Plant Physiol.* 174, 572–582. doi: 10.1104/pp.16.01772
- Buckley, T. N., Mott, K. A., and Farquhar, G. D. (2003). A hydromechanical and biochemical model of stomatal conductance. *Plant Cell Environ.* 26, 1767–1785. doi: 10.1046/j.1365-3040.2003.01094.x
- Campbell, B. W., Mani, D., Curtin, S. J., Slattey, R. A., Michno, J. M., Ort, D. R., et al. (2015). Identical substitutions in magnesium chelatase paralogs result in chlorophyll-deficient soybean mutants. *G3 (Bethesda)* 5, 123–131. doi: 10.1534/g3.114.015255
- Chukhutsina, V. U., Holzwarth, A. R., and Croce, R. (2019). Time-resolved fluorescence measurements on leaves: principles and recent developments. *Photosynth. Res.* 140, 355–369.

DATA AVAILABILITY STATEMENT

The raw data supporting the conclusions of this article will be made available by the authors, without undue reservation.

AUTHOR CONTRIBUTIONS

NS and FC wrote the manuscript. NS and GA performed the experiments. NS, FG, FC, and SM designed the model. NS, FC, and FG wrote the equations. NS implemented the model. SM and AP supervised the work. All authors agreed on the final version of the manuscript.

FUNDING

FC was funded by the project AIM1850344, of the AIM (Attraction and International Mobility) Program, financed by the Italian Ministry of Education, University and Research (MIUR).

SUPPLEMENTARY MATERIAL

The Supplementary Material for this article can be found online at: <https://www.frontiersin.org/articles/10.3389/fpls.2021.787877/full#supplementary-material>

- Cornic, G., and Baker, N. R. (2012). “Electron transport in leaves: a physiological perspective,” in *Photosynthesis*, eds J. Eaton-Rye, B. Tripathy, and T. Sharkey (Dordrecht: Springer), 591–605.
- Ebenhöh, O., Fucile, G., Finazzi, G., Rochaix, J. D., and Goldschmidt-Clermont, M. (2014). Short-term acclimation of the photosynthetic electron transfer chain to changing light: a mathematical model. *Philos. Trans. R. Soc. B Biol. Sci.* 369:20130223. doi: 10.1098/rstb.2013.0223
- Farquhar, G. D., and Von Caemmerer, S. (1982). “Modelling of photosynthetic response to environmental conditions,” in *Physiological Plant Ecology II*, eds O. L. Lange, P. S. Nobel, C. B. Osmond, and H. Ziegler (Berlin: Springer), 549–587.
- Farquhar, G. D., von Caemmerer, S. V., and Berry, J. A. (1980). A biochemical model of photosynthetic CO₂ assimilation in leaves of C₃ species. *Planta* 149, 78–90. doi: 10.1007/BF00386231
- Ferroni, L., Živčák, M., Sytar, O., Kovár, M., Watanabe, N., Pancaldi, S., et al. (2020). Chlorophyll-depleted wheat mutants are disturbed in photosynthetic electron flow regulation but can retain an acclimation ability to a fluctuating light regime. *Environ. Exp. Bot.* 178:104156. doi: 10.1016/j.envexpbot.2020.104156
- Flexas, J., Loreto, F., and Medrano, H. (eds) (2012). *Terrestrial Photosynthesis In A Changing Environment: A Molecular, Physiological, And Ecological Approach*. Cambridge: Cambridge University Press.
- Forrester, J. W. (1971). *Principle of Systems*. New York: Pegasus Communications.
- Foyer, C. H., Ruban, A. V., and Nixon, P. J. (2017). Photosynthesis solutions to enhance productivity. *Philos. Trans. R. Soc. B Biol. Sci.* 372, 3–6. doi: 10.1098/rstb.2016.0374
- García-Molina, A., and Leister, D. (2020). Accelerated relaxation of photoprotection impairs biomass accumulation in *Arabidopsis*. *Nat. Plants* 6, 9–12. doi: 10.1038/s41477-019-0572-z
- Genesio, L., Bright, R. M., Alberti, G., Peressotti, A., Delle Vedove, G., Incerti, G., et al. (2020). A chlorophyll-deficient, highly reflective soybean mutant: radiative forcing and yield gaps. *Environ. Res. Lett.* 15:074014. doi: 10.1088/1748-9326/ab865e

- Genty, B., Briantais, J. M., and Baker, N. R. (1989). The relationship between the quantum yield of photosynthetic electron transport and quenching of chlorophyll fluorescence. *Biochim. Biophys. Acta* 990, 87–92. doi: 10.1016/S0304-4165(89)80016-9
- Graham, P. J., Nguyen, B., Burdyny, T., and Sinton, D. (2017). A penalty on photosynthetic growth in fluctuating light. *Sci. Rep.* 7:12513. doi: 10.1038/s41598-017-12923-1
- Gu, J., Zhou, Z., Li, Z., Chen, Y., Wang, Z., and Zhang, H. (2017). Rice (*Oryza sativa* L.) with reduced chlorophyll content exhibit higher photosynthetic rate and efficiency, improved canopy light distribution, and greater yields than normally pigmented plants. *Field Crops Res.* 200, 58–70. doi: 10.1016/j.fcr.2016.10.008
- Holzwarth, A. R., and Jahns, P. (2014). “Non-photochemical quenching mechanisms in intact organisms as derived from ultrafast-fluorescence kinetic studies,” in *Non-Photochemical Quenching And Energy Dissipation In Plants, Algae And Cyanobacteria*, eds B. Demmig-Adams, G. Garab, W. Adams, and Govindjee (Dordrecht: Springer), 129–156.
- Jahns, P., and Holzwarth, A. R. (2012). The role of the xanthophyll cycle and of lutein in photoprotection of photosystem II. *Biochim. Biophys. Acta* 1817, 182–193.
- Johnson, J. E., and Berry, J. A. (2021). The role of Cytochrome b6f in the control of steady-state photosynthesis: a conceptual and quantitative model. *Photosynth. Res.* 148, 101–136. doi: 10.1007/s1120-021-00840-4
- Kaiser, E., Morales, A., and Harbinson, J. (2018). Fluctuating light takes crop photosynthesis on a rollercoaster ride. *Plant Physiol.* 176, 977–989. doi: 10.1104/pp.17.01250
- Kaiser, E., Morales, A., Harbinson, J., Kromdijk, J., Heuvelink, E., and Marcelis, L. F. (2015). Dynamic photosynthesis in different environmental conditions. *J. Exp. Bot.* 66, 2415–2426. doi: 10.1093/jxb/eru406
- Kannan, K., Wang, Y., Lang, M., Challa, G. S., Long, S. P., and Marshall-Colon, A. (2019). Combining gene network, metabolic and leaf-level models shows means to future-proof soybean photosynthesis under rising CO₂. *In Silico Plants* 1:diz008. doi: 10.1093/insilicoplants/diz008
- Kirschbaum, M. U. F., Küppers, M., Schneider, H., Giersch, C., and Noe, S. (1997). Modelling photosynthesis in fluctuating light with inclusion of stomatal conductance, biochemical activation and pools of key photosynthetic intermediates. *Planta* 204, 16–26. doi: 10.1007/s004250050225
- Kohzuma, K., and Hikosaka, K. (2018). Physiological validation of photochemical reflectance index (PRI) as a photosynthetic parameter using *Arabidopsis thaliana* mutants. *Biochem. Biophys. Res. Commun.* 498, 52–57.
- Kono, M., and Terashima, I. (2014). Long-term and short-term responses of the photosynthetic electron transport to fluctuating light. *J. Photochem. Photobiol. B Biol.* 137, 89–99. doi: 10.1016/j.jphotobiol.2014.02.016
- Krall, J. P., and Edwards, G. E. (1992). Relationship between photosystem II activity and CO₂ fixation in leaves. *Physiol. Plant.* 86, 180–187. doi: 10.1111/j.1399-3054.1992.tb01328.x
- Krause, G. H., Vernotte, C., and Briantais, J. M. (1982). Photoinduced quenching of chlorophyll fluorescence in intact chloroplasts and algae. Resolution into two components. *Biochim. Biophys. Acta* 679, 116–124.
- Kromdijk, J., Glowacka, K., Leonelli, L., Gabilly, S. T., Iwai, M., Niyogi, K. K., et al. (2016). Improving photosynthesis and crop productivity by accelerating recovery from photoprotection. *Science* 354, 857–861. doi: 10.1126/science.aai8878
- Li, Y. T., Yang, C., Zhang, Z. S., Zhao, S. J., and Gao, H. Y. (2021). Photosynthetic acclimation strategies in response to intermittent exposure to high light intensity in wheat (*Triticum aestivum* L.). *Environ. Exp. Bot.* 181:104275. doi: 10.1016/j.envexpbot.2020.104275
- Long, S. P., and Bernacchi, C. J. (2003). Gas exchange measurements, what can they tell us about the underlying limitations to photosynthesis? Procedures and sources of error. *J. Exp. Bot.* 54, 2393–2401. doi: 10.1093/jxb/erg262
- Matsubara, S. (2018). Growing plants in fluctuating environments: why bother? *J. Exp. Bot.* 69, 4651–4654. doi: 10.1093/jxb/ery312
- Matthews, J. S., Viallet-Chabrand, S., and Lawson, T. (2018). Acclimation to fluctuating light impacts the rapidity of response and diurnal rhythm of stomatal conductance. *Plant Physiol.* 176, 1939–1951. doi: 10.1104/pp.17.01809
- Matuszyńska, A., Heidari, S., Jahns, P., and Ebenhoeh, O. (2016). A mathematical model of non-photochemical quenching to study short-term light memory in plants. *Biochim. Biophys. Acta* 1857, 1860–1869. doi: 10.1016/j.bbabi.2016.09.003
- Morales, A., Kaiser, E., Yin, X., Harbinson, J., Molenaar, J., Driever, S. M., et al. (2018). Dynamic modelling of limitations on improving leaf CO₂ assimilation under fluctuating irradiance. *Plant Cell Environ.* 41, 589–604. doi: 10.1111/pce.13119
- Müller, P., Li, X. P., and Niyogi, K. K. (2001). Non-photochemical quenching. A response to excess light energy. *Plant Physiol.* 125, 1558–1566.
- Nedbal, L., and Lazár, D. (2021). Photosynthesis dynamics and regulation sensed in the frequency domain. *Plant Physiol.* 187, 646–661. doi: 10.1093/plphys/kiab31
- Nilkens, M., Kress, E., Lambrev, P., Miloslavina, Y., Müller, M., Holzwarth, A. R., et al. (2010). Identification of a slowly inducible zeaxanthin-dependent component of non-photochemical quenching of chlorophyll fluorescence generated under steady-state conditions in *Arabidopsis*. *Biochim. Biophys. Acta-Bioenerg.* 1797, 466–475. doi: 10.1016/j.bbabi.2010.01.001
- Norton, J. (2015). An introduction to sensitivity assessment of simulation models. *Environ. Modell. Softw.* 69, 166–174. doi: 10.1016/j.envsoft.2015.03.020
- Ort, D. R., Merchant, S. S., Alric, J., Barkan, A., Blankenship, R. E., Bock, R., et al. (2015). Redesigning photosynthesis to sustainably meet global food and bioenergy demand. *Proc. Natl. Acad. Sci. U. S. A.* 112, 8529–8536. doi: 10.1073/pnas.1424031112
- Pearcy, R. W. (1990). Sunflecks and photosynthesis in plant canopies. *Ann. Rev. Plant Biol.* 41, 421–453. doi: 10.1146/annurev.pp.41.060190.002225
- Pettersson, G., and Ryde-Pettersson, U. (1988). A mathematical model of the Calvin photosynthesis cycle. *Eur. J. Biochem.* 175, 661–672. doi: 10.1111/j.1432-1033.1988.tb14242.x
- Porcar-Castell, A., Bäck, J., Juurola, E., and Hari, P. (2006). Dynamics of the energy flow through photosystem II under changing light conditions: a model approach. *Funct. Plant Biol.* 33, 229–239. doi: 10.1071/FP05133
- Posada, J. M., Lechowicz, M. J., and Kitajima, K. (2009). Optimal photosynthetic use of light by tropical tree crowns achieved by adjustment of individual leaf angles and nitrogen content. *Ann. Bot.* 103, 795–805. doi: 10.1093/aob/mcn265
- Retkute, R., Smith-Unna, S. E., Smith, R. W., Burgess, A. J., Jensen, O. E., Johnson, G. N., et al. (2015). Exploiting heterogeneous environments: does photosynthetic acclimation optimize carbon gain in fluctuating light? *J. Exp. Bot.* 66, 2437–2447. doi: 10.1093/jxb/erv055
- Roach, T., and Krieger-Liszkay, A. (2014). Regulation of photosynthetic electron transport and photoinhibition. *Curr. Protein Pept. Sci.* 15, 351–362. doi: 10.2174/1389203715666140327105143
- Rochaix, J. D. (2011). Regulation of photosynthetic electron transport. *Biochim. Biophys. Acta* 1807, 375–383. doi: 10.1016/j.bbabi.2010.11.010
- Ruban, A. W., and Wilson, S. (2021). The mechanism of non-photochemical quenching in plants: localization and driving forces. *Plant Cell Physiol.* 62, 1063–1072. doi: 10.1093/pcp/pcaa155
- Sakowska, K., Alberti, G., Genesio, L., Peressotti, A., Delle Vedove, G., Gianelle, D., et al. (2018). Leaf and canopy photosynthesis of a chlorophyll deficient soybean mutant. *Plant Cell Environ.* 41, 1427–1437. doi: 10.1111/pce.13180
- Saltelli, A., Tarantola, S., Campolongo, F., and Ratto, M. (2004). *Sensitivity Analysis in Practice: a Guide to Assessing Scientific Models*, Vol. 1. New York, NY: Wiley
- Salvatori, N., Giorgio, A., Muller, O., Rascher, U., and Peressotti, A. (2021). A low-cost automated growth chamber system for continuous measurements of gas exchange at canopy scale in dynamic conditions. *Plant Methods* 17, 1–11. doi: 10.1186/s13007-021-00772-z
- Slattery, R. A., Grennan, A. K., Sivaguru, M., Sozzani, R., and Ort, D. R. (2016). Light sheet microscopy reveals more gradual light attenuation in light-green versus dark-green soybean leaves. *J. Exp. Bot.* 67, 4697–4709. doi: 10.1093/jxb/erw246
- Slattery, R. A., VanLooche, A., Bernacchi, C. J., Zhu, X. G., and Ort, D. R. (2017). Photosynthesis, light use efficiency, and yield of reduced-chlorophyll soybean mutants in field conditions. *Front. Plant Sci.* 8:549. doi: 10.3389/fpls.2017.00549
- Soleh, M. A., Tanaka, Y., Kim, S. Y., Huber, S. C., Sakoda, K., and Shiraiwa, T. (2017). Identification of large variation in the photosynthetic induction response among 37 soybean [Glycine max (L.) Merr.] genotypes that is not correlated with steady-state photosynthetic capacity. *Photosynth. Res.* 131, 305–315. doi: 10.1007/s1120-016-0323-1
- Soleh, M. A., Tanaka, Y., Nomoto, Y., Iwahashi, Y., Nakashima, K., Fukuda, Y., et al. (2016). Factors underlying genotypic differences in the induction of photosynthesis in soybean [Glycine max (L.) Merr.]. *Plant Cell Environ.* 39, 685–693. doi: 10.1111/pce.12674

- Song, Q., and Zhu, X. G. (2012). "A model of canopy photosynthesis in rice that combines sub-models of 3D plant architecture, radiation transfer, leaf energy balance and C3 photosynthesis," in *2012 IEEE 4th International Symposium on Plant Growth Modeling, Simulation, Visualization and Applications*, (Piscataway: IEEE), 360–366. doi: 10.1109/PMA.2012.6524858
- Stirbet, A., Lázár, D., Guo, Y., and Govindjee, G. (2020). Photosynthesis: basics, history and modelling. *Ann. Bot.* 126, 511–537. doi: 10.1093/aob/mcz171
- Taylor, S. H., and Long, S. P. (2017). Slow induction of photosynthesis on shade to sun transitions in wheat may cost at least 21% of productivity. *Philos. Trans. R. Soc. B Biol. Sci.* 372:20160543. doi: 10.1098/rstb.2016.0543
- Timm, H. C., Küppers, M., and Stegemann, J. (2004). Non-destructive analysis of architectural expansion and assimilate allocation in different tropical tree saplings: consequences of using steady-state and dynamic photosynthesis models. *Ecotropica* 10, 101–121.
- Urban, J., Ingwers, M., McGuire, M. A., and Teskey, R. O. (2017). Stomatal conductance increases with rising temperature. *Plant Signal. Behav.* 12:e1356534. doi: 10.1080/15592324.2017.1356534
- van der Tol, C., Verhoef, W., Timmermans, J., Verhoef, A., and Su, Z. (2009). An integrated model of soil-canopy spectral radiances, photosynthesis, fluorescence, temperature and energy balance. *Biogeosciences* 6, 3109–3129. doi: 10.5194/bg-6-3109-2009
- Vialet-Chabrand, S., Matthews, J. S., McAusland, L., Blatt, M. R., Griffiths, H., and Lawson, T. (2017a). Temporal dynamics of stomatal behavior: modeling and implications for photosynthesis and water use. *Plant Physiol.* 174, 603–613. doi: 10.1104/pp.17.00125
- Vialet-Chabrand, S., Matthews, J. S., Simkin, A. J., Raines, C. A., and Lawson, T. (2017b). Importance of fluctuations in light on plant photosynthetic acclimation. *Plant Physiol.* 173, 2163–2179. doi: 10.1104/pp.16.01767
- Vialet-Chabrand, S., Matthews, J. S. A., Brendel, O., Blatt, M. R., Wang, Y., Hills, A., et al. (2016). Modelling water use efficiency in a dynamic environment: an example using *Arabidopsis thaliana*. *Plant Sci.* 251, 65–74. doi: 10.1016/j.plantsci.2016.06.016
- Von Caemmerer, S. (2013). Steady-state models of photosynthesis. *Plant Cell Environ.* 36, 1617–1630. doi: 10.1111/pce.12098
- Walker, B. J., Drewry, D. T., Slattery, R. A., VanLoocke, A., Cho, Y. B., and Ort, D. R. (2018). Chlorophyll can be reduced in crop canopies with little penalty to photosynthesis. *Plant Physiol.* 176, 1215–1232. doi: 10.1104/pp.17.01401
- Yamori, W. (2016). Photosynthetic response to fluctuating environments and photoprotective strategies under abiotic stress. *J. Plant Res.* 129, 379–395. doi: 10.1007/s10265-016-0816-1
- Yamori, W., and Shikanai, T. (2016). Physiological functions of cyclic electron transport around photosystem I in sustaining photosynthesis and plant growth. *Ann. Rev. Plant Biol.* 67, 81–106. doi: 10.1146/annurev-arplant-043015-112002
- Ye, Z. P., Suggett, D. J., Robakowski, P., and Kang, H. J. (2013). A mechanistic model for the photosynthesis–light response based on the photosynthetic electron transport of photosystem II in C3 and C4 species. *New Phytol.* 199, 110–120. doi: 10.1111/nph.12242
- Zhang, H., Zhong, H., Wang, J., Sui, X., and Xu, N. (2016). Adaptive changes in chlorophyll content and photosynthetic features to low light in *Physocarpus amurensis* Maxim and *Physocarpus opulifolius* "Diabolo". *PeerJ* 4:e2125. doi: 10.7717/peerj.2125
- Zhu, X. G., Wang, Y. U., Ort, D. R., and Long, S. P. (2013). e-photosynthesis: a comprehensive dynamic mechanistic model of C3 photosynthesis: from light capture to sucrose synthesis. *Plant Cell Environ.* 36, 1711–1727. doi: 10.1111/pce.12025

Conflict of Interest: The authors declare that the research was conducted in the absence of any commercial or financial relationships that could be construed as a potential conflict of interest.

Publisher's Note: All claims expressed in this article are solely those of the authors and do not necessarily represent those of their affiliated organizations, or those of the publisher, the editors and the reviewers. Any product that may be evaluated in this article, or claim that may be made by its manufacturer, is not guaranteed or endorsed by the publisher.

Copyright © 2022 Salvatori, Carteni, Giannino, Alberti, Mazzoleni and Peressotti. This is an open-access article distributed under the terms of the Creative Commons Attribution License (CC BY). The use, distribution or reproduction in other forums is permitted, provided the original author(s) and the copyright owner(s) are credited and that the original publication in this journal is cited, in accordance with accepted academic practice. No use, distribution or reproduction is permitted which does not comply with these terms.